Swarm Level 2 Processing System

Intermediate validation of Swarm Level 2 Lithospheric Field Product

SW_OPER_MLI_VALi2C_00000000T000000_99999999T999999_0203

By: DTU

Date: 2017-04-10

Abstract and Conclusion

The processes and tests applied in the intermediate validation of the MLI_SHAi2C product

SW_OPER_MLI_SHAi2C_00000000T000000_99999999T999999_0203

and the conclusions on the product quality drawn herefrom are described in this document.

This product contains the representation of a model of the magnetic field of Earth's lithosphere ("crust") ("MLI" part of product name) using spherical harmonic coefficients ("SHA" part of product name). The model is estimated from Swarm and observatory data using the *Comprehensive Inversion* (CI) scheme within the Swarm Level 2 Processing system ("2C" part of product name). Operational Swarm Level 1b data version 0501, covering the period from 2013-12-01 to 2016-12-31 are used for the model estimation; the product is considered static i.e. valid at all times ("00000000T000000_99999999T999999" part of product name). This is version 0203 of the product (last part of product name) i.e. same baseline version (02) as the previous CI product release and hence an increase in the file counter (03). The format of the product is described in "Product Specification for L2 Products and Auxiliary Products", doc. no. SW-DS-DTU-GS-0001.

The assessment of the SW_OPER_MLI_SHAi2C_00000000T000000_99999999T999999_0203 product shows good agreement with other lithospheric field models such as MF7 [Maus, S., G3, 2010] and CHAOS-6 [Finlay, EPS, 2016].

The DTU SIL's opinion is that the MLI_SHAi2C product is validated and is therefore suitable for release.

© DTU, DK, 2017. Proprietary and intellectual rights of DTU, DK are involved in the subject-matter of this material and all manufacturing, reproduction, use, disclosure, and sales rights pertaining to such subject-matter are expressly reserved. This material is submitted for a specific purpose as agreed in writing, and the recipient by accepting this material agrees that this material will not be used, copied, or reproduced in whole or in part nor its contents (or any part thereof) revealed in any manner or to any third party, except own staff, to meet the purpose for which it was submitted and subject to the terms of the written agreement.

Table of Contents

Table of Figures

Table of Tables

Abbreviations

Acronym	*Description*
AR-2	Acceptance Review 2
CI	Comprehensive Inversion
L2PS	Level 2 Processing System
MLI	Magnetic Lithospheric field
PDGS	Payload Data Ground Segment
SHA	Spherical Harmonic Analysis
SIFM	Swarm Initial Field Model
SIL	Scientist in the Loop
STR	Star Tracker
TDS	Test Data Set
VAL	Validation
VFM	Vector Field Magnetometer

References

[Finlay, EPS, 2016] *Recent geomagnetic secular variation from Swarm and ground observatories as estimated in the CHAOS-6 geomagnetic field model*; Finlay, Christopher C.; Olsen, Nils; Kotsiaros, Stavros; Gillet, Nicolas; Tøffner-Clausen, Lars; Earth, Planets and Space, Vol 68, 112. doi: 10.1186/s40623-016-0486-1, 2016

[Maus, S., G3, 2010] *Magnetic field model MF7*; Maus, Stefan, G3, 2010

[Sabaka, GRL, 2016] *Extracting Ocean-Generated Tidal Magnetic Signals from Swarm Data through Satellite Gradiometry*; Sabaka, Terence J. ; Tyler, Robert H. ; Olsen, Nils in journal: Geophysical Research Letters (ISSN: 0094-8276) doi: 10.1002/2016GL068180, 2016

The use and/or disclosure, etc. of the contents of this document (or any part thereof) is subject to the restrictions referenced on the front page.

1 Intermediate Validation Report of MLI_SHAi2C

1.1 Input data products

The following input data products were used for the estimation of the MLI_SHAi2C lithospheric field model

Products	Type	Period	Comment
SW_OPER_Q3D_CI_i2__00000000T000000_99999999T999999_0101	Q-matrix of Earth's (1-D mantle + oceans)	-	Used for computing induced part of ionospheric field
SW_OPER_AUX_OBS_2__20130101T000000_20131231T235959_0109 SW_OPER_AUX_OBS_2__20140101T000000_20141231T235959_0109 SW_OPER_AUX_OBS_2__20150101T000000_20151231T235959_0109 SW_OPER_AUX_OBS_2__20160101T000000_20161231T235959_0109	Observatory hourly mean values	2013-12-01 – 2016-10-31	A total of 143 observatories are included
SW_OPER_AUX_DST_2__19980101T013000_20170103T233000_0001 SW_OPER_AUX_F10_2__19980101T000000_20170101T000000_0001 SW_OPER_AUX_KP__2__19990101T023000_20161215T223000_0001	Indices	As indicated by the file names	
SW_OPER_MAGA_LR_1B_*yyyymmddTh1m1s1_yyyymmddTh2m2s2*_0501 SW_OPER_MAGB_LR_1B_*yyyymmddTh1m1s1_yyyymmddTh2m2s2*_0501 SW_OPER_MAGC_LR_1B_*yyyymmddTh1m1s1_yyyymmddTh2m2s2*_0501	Swarm magnetic data, 1 Hz	2013-12-01 - 2016-12-31	Decimated to 15 second sampling

Table 1-1: Input data products

1.2 Model Parameterization and Data Selection

See Section 2.1.

1.3 Output Products

The products of this validation report are:

Swarm Level 2 Magnetic Lithospheric field Product:

SW_OPER_MLI_SHAi2C_00000000T000000_99999999T999999_0203

Swarm Level 2 Intermediate Validation Product:

SW_OPER_MLI_VALi2C_00000000T000000_99999999T999999_0203

1.4 Validation Results

The tests were conducted between 2017-02-14 and 2017-03-02.

The following tests have been applied to the lithospheric model output product. See Annex A for general definitions of various tests.

The use and/or disclosure, etc. of the contents of this document (or any part thereof) is subject to the restrictions referenced on the front page.

1.4.1 Spectral Power Density

Figure 1-1 below shows the spectral power density of the CI, CHAOS-6, and MF-7 lithospheric field models in blue and dashed black respectively green; and the power of the differences between the CI model and CHAOS-6 (red) and MF7 (cyan). The differences are everywhere below the actual field; but as of degree 85, the power of the CI model is somewhat larger than that of the other models indicative of measurement noise starting to impact the model.

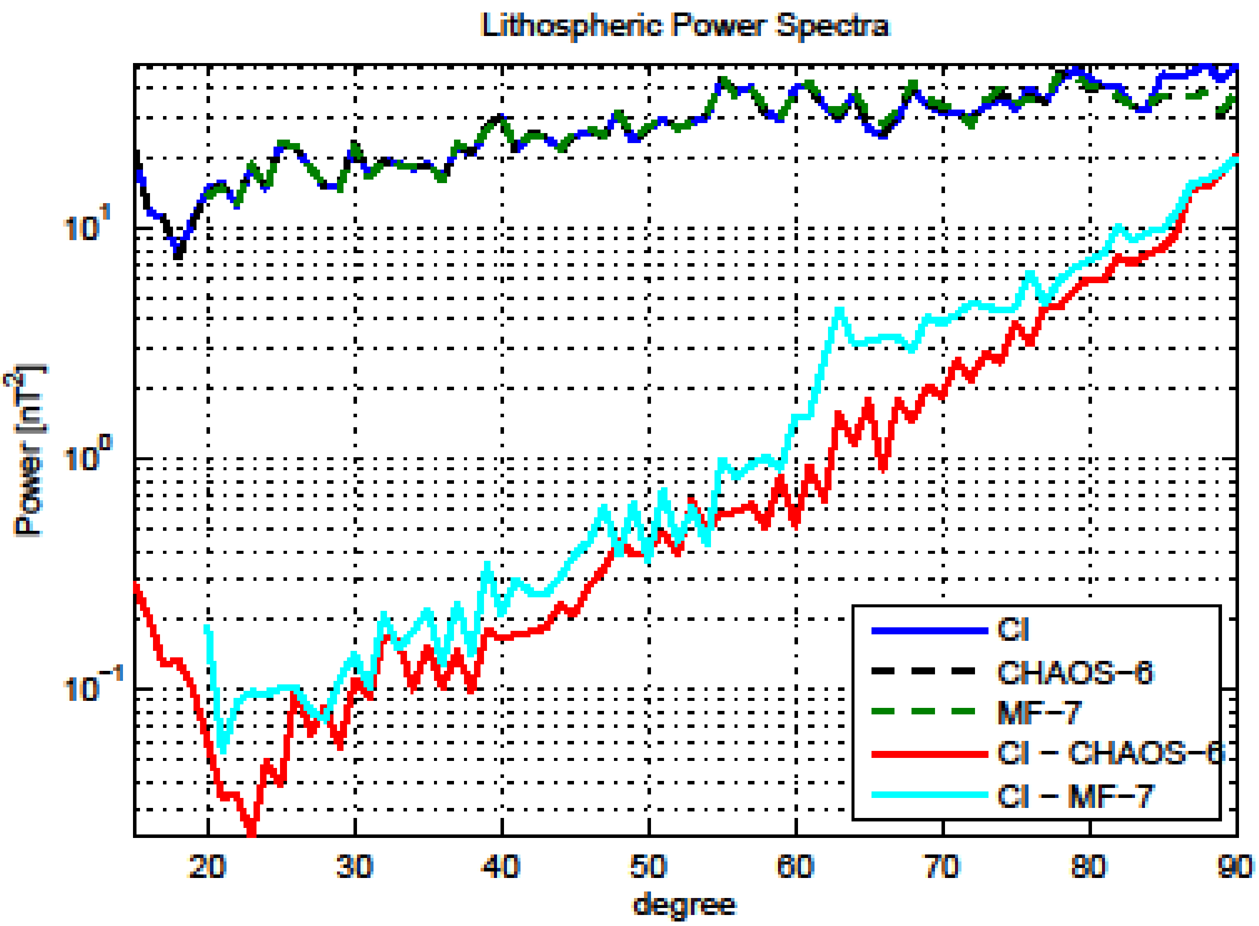

Figure 1-1: Spectral power densities, lithospheric field, at Earth's surface, epoch 2015

1.4.2 Spherical Harmonic Degree Correlation

Figure 1-2 to the right shows the degree correlation between the CI model and the other models. Again the good agreement between the models is confirmed by the correlations being above 0.8 for all degrees but 90.

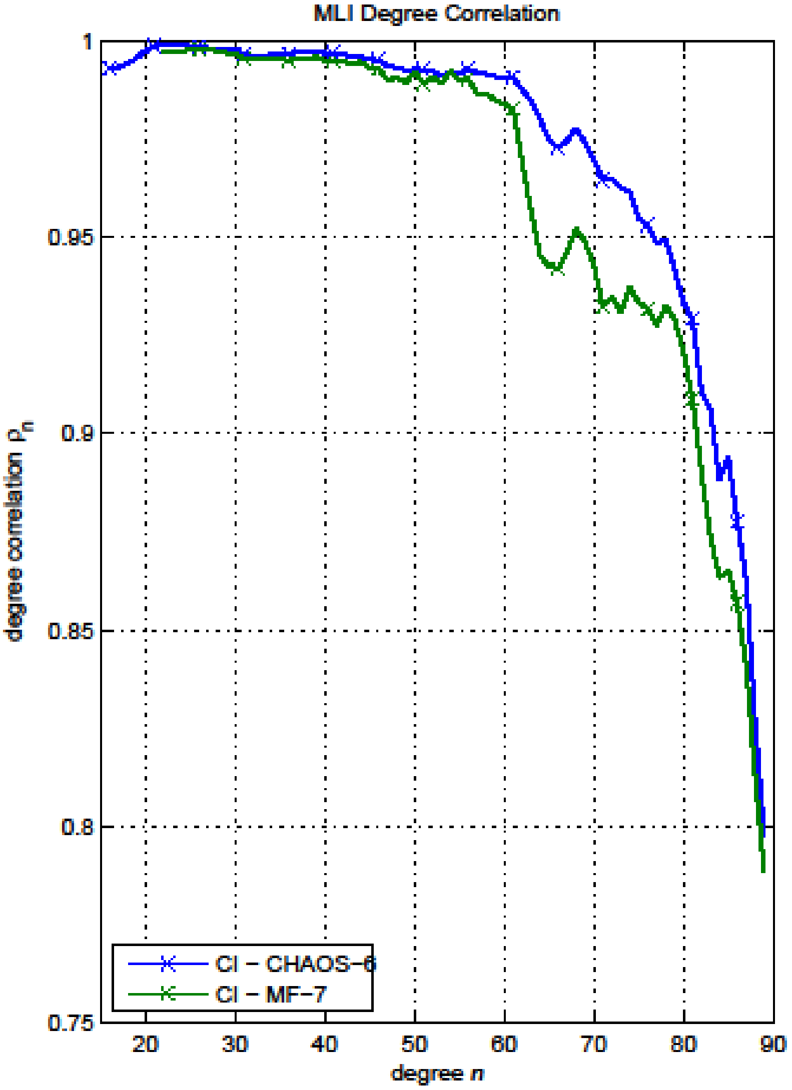

Figure 1-2: Lithospheric field model, degree correlation

1.4.3 Normalized Spherical Harmonic Coefficient Differences

Figure 1-3 below shows the relative differences in percent between each spherical harmonic coefficient of the CI and the CHAOS-6 and MF7* models respectively in degree versus order matrices. These plots show some differences at lower degree and low order probably due to crosstalk with the ionospheric field.

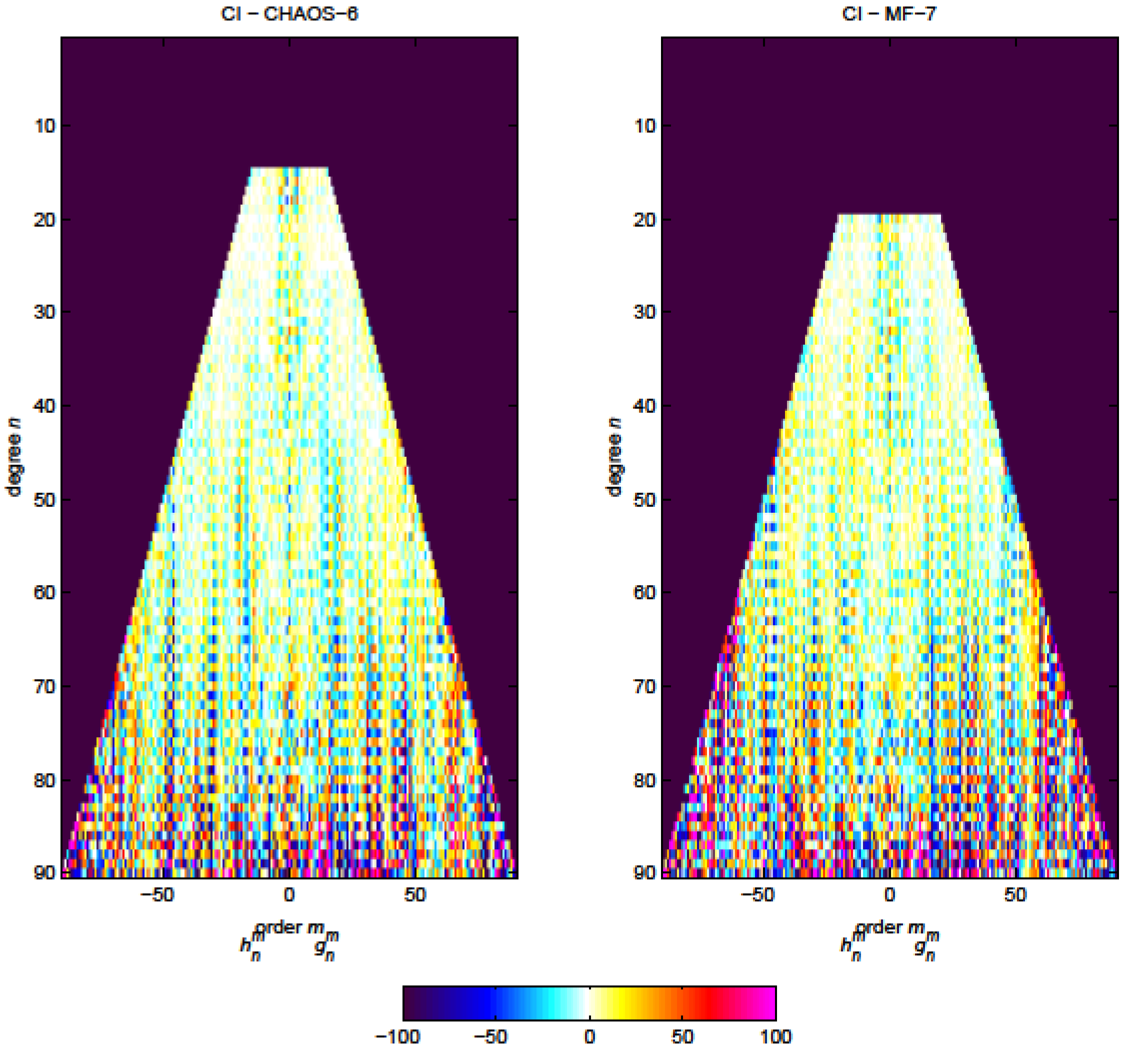

Figure 1-3: Normalized coefficient differences in percent

* Degrees 20-90

The use and/or disclosure, etc. of the contents of this document (or any part thereof) is subject to the restrictions referenced on the front page.

1.4.4 Visualisation of spatial differences

Figure 1-4 below shows the difference in B_r between the CI and CHAOS-6 lithospheric field models at Earth's surface for degrees 15-90 at epoch 2015. These plots reveal the main differences to be concentrated around the magnetic poles but also show a slight tendency to "banding" along the satellite tracks.

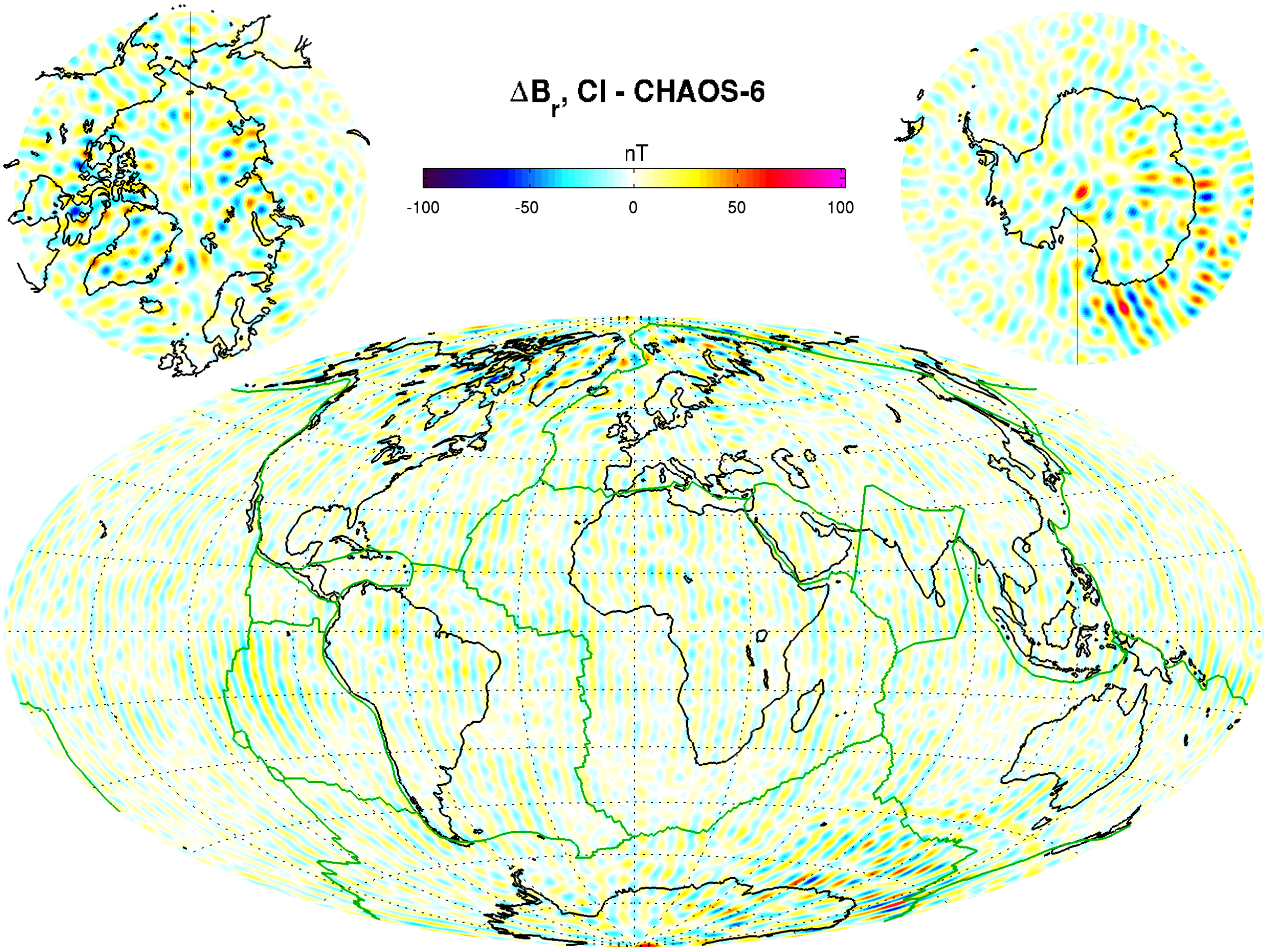

Figure 1-4: Spatial visualization of B_r differences between CI and CHAOS-6 models

1.4.5 Visualisation of radial field

Figure 1-5 below shows the radial field, B_r, of the CI lithospheric field models at Earth's surface for degrees 15-90 at epoch 2015 (using a square-root scale to visually enhance the weak signals in some regions).

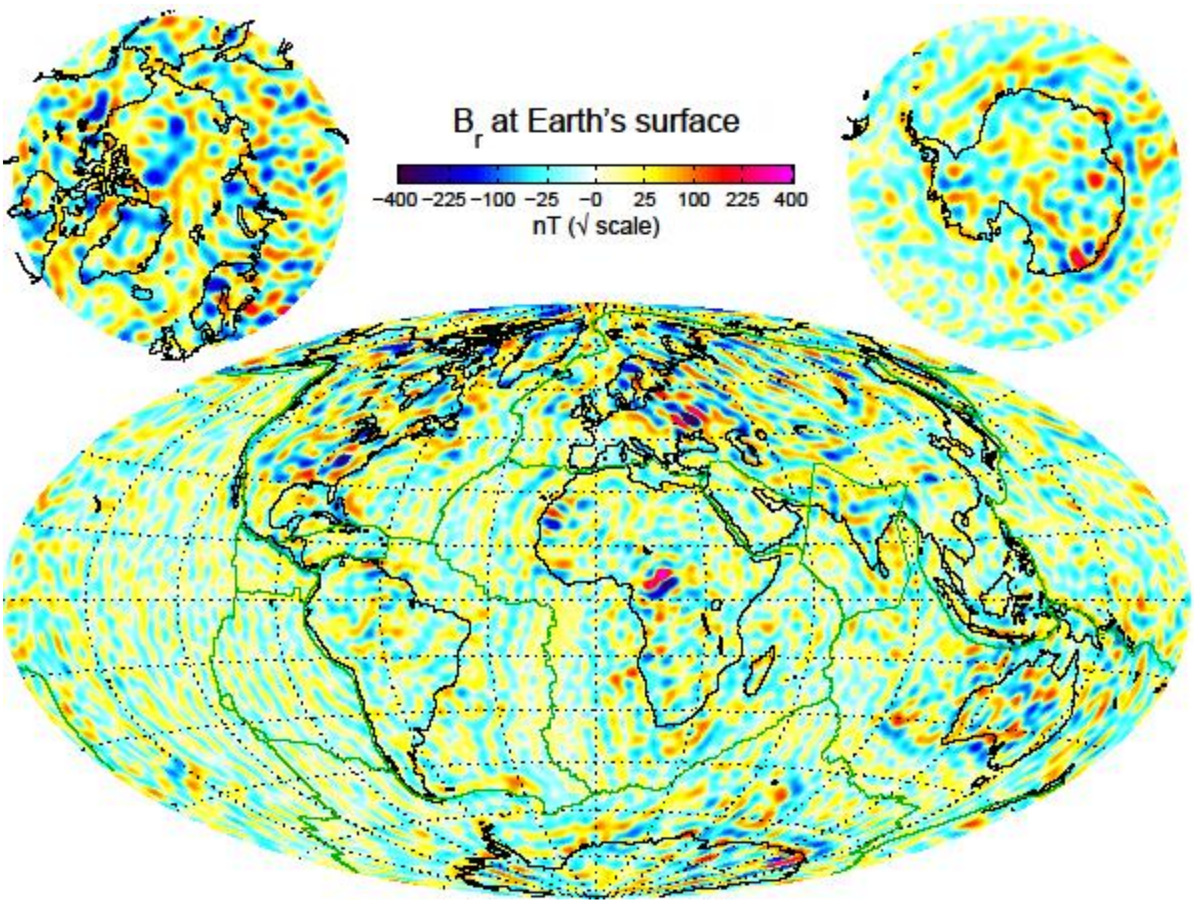

Figure 1-5: Spatial visualization of B_r of the CI model

1.4.6 Data Statistics

The statistics of the data residuals obtained by the CI modelling is given in Table 1-2 below. Grey cells indicate data from night side, white cells indicate data from sunlit regions. Crossed cells indicate data which are not used in the inversion process. "Field" indicate the pure vector and scalar measurements, whereas "NS diff" and "EW diff" indicate the North-South (along-track) respectively East-West differences. The standard deviations (of the residuals between the observations and the estimated model) of the differences are quite impressive; the standard deviations of the direct field measurements from the satellites are also quite excellent whereas the ground observatories show slightly higher residuals than previously recorded. Note also the expected similarity between Swarm A and C (side-by-side flying pair) and North-South differences for all three satellites. Swarm B shows slightly higher residuals in the Field components at low and mid latitudes and slightly lower residuals at high latitudes likely due to its higher altitude.

Swarm/ Obs.		Geomagnetic quasi-dipole latitude											
		Low, ≤ 10°				Mid,]10°..55°]				High, > 55°			
		Standard deviations of data residuals, weighted, [nT]											
		σ(B_r)	σ(B_θ)	σ(B_φ)	σ(F)	σ(B_r)	σ(B_θ)	σ(B_φ)	σ(F)	σ(B_r)	σ(B_θ)	σ(B_φ)	σ(F)
A	Field	1.77	3.30	1.98	3.21	2.73	3.62	2.86	2.06				5.97
	NS diff	0.38	0.18	0.37	0.19	0.26	0.33	0.39	0.20				1.84
		1.30	0.98	1.20	0.85	0.61	0.72	1.27	0.33				2.59
B	Field	1.95	4.07	2.84	4.00	3.14	4.48	3.77	2.71				5.78
	NS diff	0.38	0.18	0.36	0.19	0.26	0.34	0.40	0.22				1.61
		1.10	0.79	1.06	0.66	0.58	0.68	1.21	0.31				2.28
C	Field	1.78	3.33	2.02	3.27	2.79	3.66	2.83	2.11				5.98
	NS diff	0.40	0.19	0.38	0.19	0.28	0.35	0.41	0.21				1.85
		1.30	0.98	1.21	0.89	0.63	0.74	1.29	0.33				2.59
A-C	EW diff	0.83	0.36	0.99	0.29	0.43	0.49	0.94	0.28				0.62
		2.10	0.78	2.52	0.55	0.96	1.10	1.64	0.44				0.75
Magnetic observatories		5.70	5.32	4.43	4.81	5.55	5.14	4.44	4.79	16.82	14.01	10.53	17.61
		12.38	13.02	10.88	11.79	8.32	8.93	10.15	8.39	23.42	22.58	16.94	26.04

Table 1-2: Observation Statistics

1.5 Criteria

Table 1-3 below summarizes the criteria used to check the validity of the MLI_SHAi2C product:

Input	**Test**	**Criteria**	**Pass?**
Observations	Residual statistics	Standard deviation of vector data below 7 nT.	Ok
Alternative model	Comparison with model	CI model agrees with alternative model	Ok

Table 1-3: Validation criteria

The use and/or disclosure, etc. of the contents of this document (or any part thereof) is subject to the restrictions referenced on the front page.

2 Additional Information

2.1 Model Configuration and Data Selection Parameters

The MLI_SHAi2C product is obtained as a comprehensive co-estimation of the core, lithosphere, ionosphere, and magnetosphere field contributions including induced contributions similar to the method described in [Sabaka, GRL, 2016]. The complete model configuration used is given in Table 2-1 below; the MLI_SHAi2C product is the green part:

Model Part	**Maximum Degree/Order**	**Temporal Characteristics**	**Comment**
Core	16/16	Order 5 B-spline with knots every 6 months	Damping of the mean-square, second and third time derivatives of B_r at the core-mantle boundary (at 3480 km radius).
Lithosphere	90/90	Static	Degree 17-90 purely determined by North-South differences from all satellites and East-West differences of lower pair satellite (A and C). Damping of B_r at the poles to reduce effect of lack of data at the poles ("*polar gap*")
Ionosphere	45/5 (dipole coordinates)	Annual, semi-annual, 24-, 12-, 8- and 6- hours periodicity	Spherical harmonic expansion in quasi-dipole (QD) frame, underlying dipole SH n_{max} = 60, m_{max} = 12. Scaling by 3-months averages of F10.7 plus induction via a priori 3-D conductivity model ("1-D+oceans") and infinite conductor at depth. Damping of: 1. Mean-square current density J in the E-region within the nightside sector (magnetic local times 21:00 through 05:00) 2. Mean-square of the surface Laplacian of J multiplied by a factor of $\sin^8(2\theta)$ over all local times, where θ is co-latitude.

The use and/or disclosure, etc. of the contents of this document (or any part thereof) is subject to the restrictions referenced on the front page.

Model Part	Maximum Degree/Order	Temporal Characteristics	Comment
Magnetosphere, external	3/1	One hour bins	
Magnetosphere, induced	3/3	One hour bins	
M2 Tidal	36/36	Periodicity: 12.42060122 hr, phase fixed with respect to 00:00:00, 1999 January 1 GMT	

Table 2-1: Model Configuration

The data selection criteria are:

- Coarse agreement with CHAOS-6 field model: $\Delta B_c \leq 500$ nT for all components $c=r,\vartheta,\varphi$, and $\Delta F \leq 100$ nT.
- $Kp \leq 3^0$
- Time-derivative of Dst: $|dDst/dt| \leq 3$ nT/hour
- 15 second satellite sampling period
- core and tidal fields determined from night-side data only, i.e. with Sun ≥ 10° below the horizon

2.2 Comments from Scientists in the Loop

2.2.1 Derivation of Model

The final Comprehensive Inversion model using three years of Swarm data shows good agreement with alternative models and very good residual statistics (Table 1-2). Slight along-track banding and differences in polar regions are observed when comparing to other models (see Figure 1-4).

2.2.2 Conclusion

The estimated model is assessed to be of good quality with very good agreement with alternative lithospheric field models.

The use and/or disclosure, etc. of the contents of this document (or any part thereof) is subject to the restrictions referenced on the front page.

Annex A Definitions of Tests

A.1 Mean square vector field difference per spherical harmonic degree

The mean square vector field difference between models per spherical harmonic degree (*n*) is diagnostic of how closely the models match on average across the globe. The difference between Gauss coefficients g_n^m of model *i* and model *j* can be defined as:

$$ {}_{i,j}R_n = (n+1)\left(\frac{a}{r}\right)^{(2n+4)} \sum_{m=0}^{n} \left[{}_i g_n^m - {}_j g_n^m \right]^2 $$

Equation A-1

where *n* is the degree, *m* is the order, *a* is the magnetic reference spherical radius of 6371.2 km which is close to the mean Earth radius, and *r* is the radius of the sphere of interest, which is taken as r = a for comparisons at the Earth's surface and r = 3480 km for comparisons at the core-mantle boundary.

Summing over degrees n from 1 to the truncation degree N and taking the square root yields the RMS vector field difference between the models *i* and *j* averaged over the spherical surface:

$$ {}_{i,j}R = \sqrt{\sum_{n=1}^{N} {}_{i,j}R_n} $$

Equation A-2

A.2 Correlation per spherical harmonic degree

Analysis of spherical harmonic spectra is a powerful way to diagnose differences in amplitude between models but tells us little about how well they are correlated. The correlation per degree between two models again labelled by the indices *i* and *j* can be studied as a function of spherical harmonic degree using the quantity: ${}_{i,j}\rho_n$

$$ {}_{i,j}\rho_n = \frac{\sum_{m=0}^{n} \left({}_i g_n^m \, {}_j g_n^m \right)}{\sqrt{\left(\sum_{m=0}^{n} \left({}_i g_n^m \right)^2 \right) \left(\sum_{m=0}^{n} \left({}_j g_n^m \right)^2 \right)}} $$

Equation A-3

Ideally, the correlation should be close to 1 for all models, indicating that they have equivalent features and coefficients. If the correlation falls below 0.5, for degrees 1-9, then the models should be examined in more detail. Coefficients from degree 10-13 in IGRF and WMM are less well-determined (e.g. due to noise) and also change more rapidly so are not expected to be well correlated by the launch of the Swarm mission.

A.3 Visualisation of coefficient differences

A final method of visualising the differences in Gauss coefficients is to plot the differences ${}_i g_n^m - {}_j g_n^m$ as a triangular plot, with the zonal coefficients lying along the centre of the triangle, the sectorial coefficients along the edges and the tesseral coefficients filling the central regions. These plots will illustrate which, if any, coefficients are strongly divergent between models

The use and/or disclosure, etc. of the contents of this document (or any part thereof) is subject to the restrictions referenced on the front page.

A.4 Visualisation of spatial differences

A geographical investigation of the models can be made by plotting the differences in the B_x, B_y and B_z components of the field at radius r = a. Studying differences between the Swarm models and reference models in space yields insight into the geographical locations where disparities are located, illustrating whether biases or errors have arisen in certain regions (e.g. polar areas).

.

The use and/or disclosure, etc. of the contents of this document (or any part thereof) is subject to the restrictions referenced on the front page.